HNPS Advances in Nuclear Physics

Vol 26 (2018)

HNPS2018

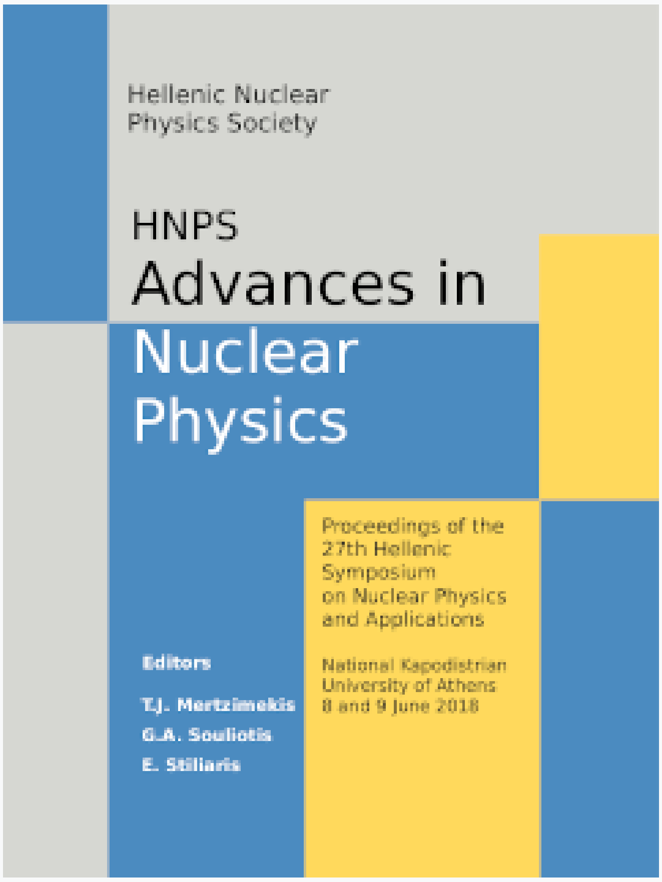

An improved method to determine neutron fluence in high energy medical accelerators using activation detectors

K. Papadopoulos, G. Siltzovalis, M. I. Savva, T. Vasilopoulou, P. Georgolopoulou, P. Karaiskos, J. Kalef-Ezra, I. E. Stamatelatos

doi: [10.12681/hnps.1830](https://doi.org/10.12681/hnps.1830)

An improved method to determine neutron fluence in high energy medical accelerators using activation detectors

K. Papadopoulos[1,3], G. Siltzovalis[1,2], M.I. Savva[1], T. Vasilopoulou[1]
P. Georgolopoulou[4], P. Karaiskos[3], J. Kalef-Ezra[2] and I.E. Stamatelatos[1]

[1] *Institute of Nuclear and Radiological Sciences, Energy, Technology & Safety, NCSR "Demokritos"*
[2] *Medical Physics Laboratory, Medical Department, University of Ioannina*
[3] *Medical Physics Laboratory, Medical School, University of Athens*
[4] *Department of Medical Physics, General Anticancer-Oncologic Hospital of Athens 'Saint Savvas'*

Abstract Scope of the present work was to test the hypothesis that a generic simulation geometry can adequately describe a high energy medical accelerator head for the purpose of estimating the parasitic neutron fluence levels at the position of the isocenter. The experiment was performed using an Elekta Synergy 18 MV linear accelerator. Gold, cobalt, indium and copper activation foils were used. Activation measurements were performed using a calibrated HPGe detector based spectrometry system. Four generic accelerator head models were considered. Neutron spectrum averaged cross-section data for each foil were derived for the examined configurations using the Monte Carlo code MCNP5 in conjuction with cross section data obtained from the International Reactor Dosimetry and Fusion File (IRDFF). It was concluded that the accelerator head can be adequately described either as a solid tungsten sphere of 10 cm radius or a spherical tungsten shell 20 cm in external diameter and 10 cm in thickness. This work contributes towards the development of a simple and computationally cost effective method for the determination of neutron fluence around high energy medical accelerators and therefore the optimization of the radiation protection of the patients and staff in radiation therapy.

Keywords neutron dosimetry, radiation therapy, radiation shielding design

INTRODUCTION

Medical accelerators operating above 8 MV result in photonuclear and electronuclear reactions in the accelerator head components, such as the target, flattening filter, primary collimators, jaws and head shielding, as well as in the patient body and the shielding materials. The produced neutrons are scattered and moderated within the treatment room and have to be taken into consideration in the design of the bunker. Moreover, they result in an increase in the out-of-field radiation dose to the irradiated patients. Therefore, the knowledge of the neutron fluence at the isocenter of the accelerator is an important parameter for the optimization of the bunker shield and the estimation of the peripheral dose to the patient.

Scope of the present work was to test the hypothesis proposed by other scientists [1-4] that a generic simulation geometry can adequately describe a high energy medical accelerator head for the purpose of estimating the parasitic neutron fluence levels at the isocentre.

EXPERIMENTAL

Irradiations were performed using an ELEKTA SYNERGY 18 MV accelerator at Saint Savvas Hospital, Athens. Neutron fluence measurements were performed at a distance of 60 cm from the target using gold, cobalt, indium and copper activation foils. During the irradiation the accelerator jaws were closed (beam area 0 cm x 0 cm). In total 30 kMU were given. The foils were positioned on a thin aluminum holder (in air).

The induced activity was assessed using a germanium detector spectrometry system of 85% relative efficiency and FWHM of 1.82 keV at 1332.5 keV. This system consists of a shielded, coaxial germanium detector (EG & G ORTEC), a digital signal acquisition and data acquisition system (DSPEC™) and a support bracket for sample positioning during measurement. Spectrum analysis was performed using the Gamma-Vision™ software. The detector was calibrated with respect to energy and full energy peak efficiency using a set of standard sources. Neutron fluence was determined using the following expression:

$$\Phi = \frac{1}{\sigma_{eff}} \cdot \frac{C \cdot \lambda}{\varepsilon \cdot I_\gamma \cdot G_\gamma \cdot f_{tcc}} \cdot \frac{1}{\cdot e^{(1-\lambda t_{irr})}} \frac{1}{e^{-\lambda t_d}} \frac{1}{e^{(1-\lambda t_c)}} \qquad (1)$$

where, ε is full energy peak efficiency, C is net counts at the photo-peak, I_γ is the γ yield, f_{tcc} is the true coincidence correction factor, G_γ is the gamma self-shielding factor, λ the decay constant, t_c is the counting time, t_{irr} is the irradiation time, t_d is the cooling time between the end of irradiation and the start of the measurement and σ_{eff} is the effective cross section for the nuclear reaction of interest. The effective cross section was defined as

$$\sigma_{eff} = \frac{\int_0^{E_{max}} \sigma(E) \cdot \Phi(E) dE}{\int_0^{E_{max}} \varphi(E) dE} \qquad (2)$$

and it was calculated for the specific nuclear reaction in the foil taking into consideration the MCNP predicted neutron fluence spectrum at the position of measurement.

SIMULATIONS

Simulations were performed using Monte Carlo code MCNP5 [5]. The accelerator head geometries studied are shown in Table 1. It is noted that, in order to accurately represent the neutron scatter component from the floor and walls at the position of the measurement, the model incorporated a detailed representation of the bunker shielding configuration including the walls, floor and ceiling as well.

The neutron energy spectrum at the source was taken from Tosi et al [6]:

$$\mathrm{n(E)} = \mathrm{a}\frac{\mathrm{E}}{\mathrm{T}^2}\exp\left(-\frac{\mathrm{E}}{\mathrm{T}}\right) + \beta \frac{\ln\left|\frac{E_{max}}{E+S_n}\right|}{\int_0^{E_{max}-S_n} \ln\left|\frac{E_{max}}{E+S_n}\right| dE} \qquad (3)$$

where α, represents the fraction of evaporation neutrons (α=0.8929), β represents the fraction of knock-on neutrons (β=0.1071), T is the temperature of the target nuclei (T=0.5 MeV) , E_{max} is the maximum energy of the accelerated electrons (E=18 MeV) and S_n is the neutron binding energy (S_n=7.34 MeV for tungsten).

Table 1. Accelerator head geometries studied

	Geometry	Material	Reference
A	point source in the center of a spherical shell of 20 cm external and 10 cm internal radius	W	Vega-Carillo et al [1]
B	point source in the center of a spherical shell of 20 cm external and 10 cm internal radius	Cu	Agosteo et al [2]
C	point source in the center of a spherical shell of 25 cm external and 10 cm internal radius	Pb	Agosteo et al [3]
D	solid sphere source with 10 cm radius	W	Carinou et al [4]

Neutron spectrum averaged cross-section data for the four generic accelerator head simulation geometries were derived for each foil using the International Reactor Dosimetry and Fusion File (IRDFF v.1.05) (Table 2).

Table 2. Calculated spectrum averaged cross sections for the different source geometries

Foil	**Reaction**	σ_{eff} (b) Vega-Carillo 2007	Agosteo 1992	Agosteo 1995	Carinou 1999
Cu	^{63}Cu(n,γ) ^{64}Cu	$(1.68 \pm 0.04)\cdot10^{-3}$	$(1.54 \pm 0.05)\cdot10^{-3}$	$(1.74 \pm 0.08)\cdot10^{-3}$	$(1.63 \pm 0.05)\cdot10^{-3}$
Au	^{197}Au(n,γ) ^{198}Au	$(6.24 \pm 0.48)\cdot10^{-4}$	$(9.51 \pm 0.93)\cdot10^{-4}$	$(1.24 \pm 0.10)\cdot10^{-3}$	$(6.83 \pm 0.47)\cdot10^{-4}$
Au(Cd)		$(4.73 \pm 0.44)\cdot10^{-4}$	$(5.06 \pm 0.50)\cdot10^{-4}$	$(8.46 \pm 0.71)\cdot10^{-4}$	$(6.04 \pm 0.60)\cdot10^{-4}$
In	^{115}In(n,γ)^{116m}In	$(7.99 \pm 0.21)\cdot10^{-3}$	$(9.07 \pm 0.37)\cdot10^{-3}$	$(9.40 \pm 0.33)\cdot10^{-3}$	$(9.25 \pm 0.36)\cdot10^{-3}$
In(Cd)		$(3.10 \pm 0.17)\cdot10^{-3}$	$(2.78 \pm 0.18)\cdot10^{-3}$	$(3.44 \pm 0.24)\cdot10^{-3}$	$(2.81 \pm 0.21)\cdot10^{-3}$
Co	^{59}Co(n,γ)^{60}Co	$(9.45 \pm 0.20)\cdot10^{-3}$	$(1.09 \pm 0.03)\cdot10^{-2}$	$(1.21 \pm 0.03)\cdot10^{-2}$	$(1.15 \pm 0.03)\cdot10^{-2}$
Mn	^{55}Mn(n,γ)^{56}Mn	$(3.10 \pm 0.16)\cdot10^{-4}$	$(3.96 \pm 0.19)\cdot10^{-4}$	$(3.78 \pm 0.14)\cdot10^{-4}$	$(3.87 \pm 0.21)\cdot10^{-4}$

RESULTS AND DISCUSION

The neutron fluence per X-ray Gray determined at the isocentre (100 cm from the target) for the different types of foils and for the different source geometries is presented in Table 3. The deviation between the fluence values obtained using different foils was considered as a critical factor and an index of suitability for the modeling of the linac head geometry. From Table 3 it can be observed that the minimum coefficient of variation was obtained from the source geometries A (6.1%) and D (8.6%), proposed by Vega-Carillo et al and Carinou et al, respectively (Fig. 1).

This work contributes towards the development of a simple and computationally cost effective method for the determination of neutron fluence around high energy medical accelerators and therefore optimizing the radiation protection of the patients and staff in radiation therapy.

Table 3. Neutron fluence at the isocenter per X-ray Gray

Foil	Φ(cm^{-2}·Gy^{-1}) x 10^7			
	Vega-Carillo 2007	Agosteo 1992	Agosteo 1995	Carinou 1999
Cu	1.21 ± 0.11	1.32 ± 0.12	1.17 ± 0.12	1.25 ± 0.12
Au	1.29 ± 0.16	0.85 ± 0.11	0.65 ± 0.08	1.18 ± 0.14
Au(Cd)	1.28 ± 0.17	1.20 ± 0.17	0.72 ± 0.09	1.00 ± 0.14
In	1.23 ± 0.14	1.08 ± 0.13	1.04 ± 0.12	1.06 ± 0.13
In(Cd)	1.22 ± 0.15	1.37 ± 0.17	1.10 ± 0.14	1.35 ± 0.18
Co	1.07 ± 0.10	0.92 ± 0.09	0.83 ± 0.08	0.87 ± 0.08
Mn	1.01 ± 0.11	0.79 ± 0.08	0.82 ± 0.09	0.81 ± 0.09
Mean	1.20 ± 0.07	1.09 ± 0.19	0.82 ± 0.20	1.13 ± 0.10
CV (%)	6.1	17.1	25.0	8.6

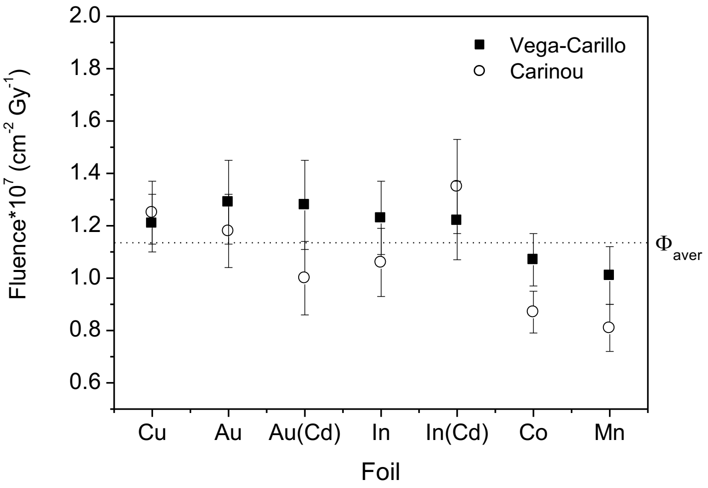

Fig. 1 Neutron fluence results per foil for the two selected geometries

ACKNOWLEGMENTS

Mr. K. Papadopoulos is a post-graduate student at the Inter-University Post-Graduate Course in Medical Radiation Physics jointly organized by the Universities of Athens, Ioannina, Thessaloniki, Crete and Thrace, GAEC and in collaboration with NCSR Demokritos. The present work was part of his post-graduate diploma thesis.

References

[1] Vega-Carillo et al, Rad. Meas., 42 (2007) 413-419
[2] Agosteo, S., et al, 1992, Nucl. Instr. Meth. Phys. Res, B, 72 (1992) 84-90
[3] Agosteo, S., et al, Health Phys., 68 (1995) 27-34.
[4] Carinou et al, Med. Phys., 12 (1999) 2520-2525
[5] X-5 Monte Carlo Team, 'MCNP - A General Monte Carlo N-Particle Transport Code', Version 5, LA-UR-03-1987, April 2003
[6] Tosi et al, Med. Phys., 18 (1991) 54-60